

ORIGINAL ARTICLE

Spreading of Tau Pathology in Sporadic Alzheimer's Disease Along Cortico-cortical Top-Down Connections

Heiko Braak and Kelly Del Tredici

Clinical Neuroanatomy Section/Department of Neurology, Center for Biomedical Research, University of Ulm, Helmholtzstrasse 8/1, 89081 Ulm, Germany

Address correspondence to Prof. Heiko Braak, MD, Clinical Neuroanatomy Section/Department of Neurology, Center for Biomedical Research, University of Ulm, Helmholtzstrasse 8/1, 89081 Ulm, Germany. Email: heiko.braak@uni-ulm.de

Abstract

By using AT8-immunocytochemistry that visualizes hyperphosphorylated tau protein, we examined neurofibrillary changes related to sporadic Alzheimer's disease (AD) in $N = 40$ individuals at neurofibrillary tangle (NFT) stages I–IV. We report the presence of abnormal tau changes within solitary pyramidal neurons in layers III and V of the neocortex. These pyramidal cells showed pathology in different cell compartments (dendritic, somatic, axonal) that appeared to occur sequentially: Tau pathology was seen in distal segments of the basal dendrites, then in proximal dendrites, the soma, and, finally, in the axon of affected neurons. These findings are remarkable in that they point to the existence of neurofibrillary changes in regions routinely associated with later NFT stages. In addition, they lend support to the idea that it may be the axons of cortico-cortical top-down neurons in neocortical fields involved in AD that carry and spread abnormal tau seeds in a focused manner (transsynaptically) into the distal dendritic segments of nerve cells following directly in the neuronal chain, thereby sustaining further tau-seeded templating.

Key words: Alzheimer's disease, hyperphosphorylated tau, neurofibrillary changes, tau seeding, top-down cortico-cortical connections

Introduction

The gradual and progressive development of aggregated tau protein in select neuronal types of the brain is central to the pathological process underlying sporadic Alzheimer's disease (AD) (Braak and Braak 1991a; Hyman and Gómez-Isla 1994; Braak and Del Tredici 2015a). The neurofibrillary lesions commence in nerve cells at defined subcortical and cortical predilection sites and progress from there according to a predictable sequence into previously uninvolved regions. In AD, the cerebral cortex bears brunt of the tau pathology: Cortical lesions begin in transition fields between allocortical and neocortical regions of the temporal lobe. From there, they progress into neocortical areas of the temporal lobe. The process then spreads into parietal and occipital high-order sensory

association fields and prefrontal areas, then into first order sensory association fields and premotor areas, and, finally, into the neocortical primary fields (Braak and Braak 1991a; Alafuzoff et al. 2008; Braak and Del Tredici 2015a). The basic construction of the various neocortical fields and their neuronal constituents have common traits, including specific cell types, laminar connections, and columnar organization (Nieuwenhuys 1994; Zilles and Amunts 2012; Amunts and Zilles 2015). The regional progression phenomenon of the pathological process in the neocortex during AD underpins our earlier proposal that the disease process might be driven by the transmission of abnormal tau seeds from a donor neuron to the next recipient neuron via cortico-cortical top-down connections (Braak and Del Tredici 2011, 2015a).

With the exception of neurofibrillary tangle (NFT) stage VI, the other stages display neocortical fields that typically are AT8-immunonegative, i.e., macroscopically uninvolved (Fig. 1). However, by using a section thickness of 100–300 μm , we could visualize and study single AT8-immunopositive pyramidal neurons, including their dendritic trees (Braak and Braak 1991b), in neocortical layers III and V of, among others, the peristriate region or the superior temporal gyrus, in individuals with neurofibrillary lesions corresponding to NFT stages I–IV. These rare AT8-immunopositive pyramidal cells were remarkable because (1) they occurred in neocortical brain regions that routinely are associated with NFT stages V and VI rather than with earlier stages (Braak and Braak 1991a; Braak et al. 2006; Alafuzoff et al. 2008; Braak and Del Tredici 2015a) and (2) they were distantly located from fields with pronounced AT8-immunoreactivity. The existence of such isolated involved pyramidal cells is in line with a recent study, in which tau seeding activity at NFT stage III anticipated tau pathology in the superior temporal gyrus and in the primary visual neocortex, regions that usually are uninvolved at this stage (Kaufman et al. 2018).

We describe new histological findings and discuss them in relationship to the manner in which the fields of the neocortex “communicate” with each other, and we also discuss the possible consequences for the progression of the pathological process underlying AD in a prion-like manner along top-down cortico-cortical connectivities.

Material and Methods

Study Cohort

Forty ($N = 40$) cases staged according to previously published protocols (Braak et al. 2006; Hyman et al. 2012) and 13 ($N = 13$) controls characterized by absence of mature neurofibrillary changes in the cerebral cortex were included. This

retrospective study was performed in compliance with university ethics committee guidelines as well as German federal and state law governing human tissue usage. Informed written permission was obtained from all patients and/or their next of kin for autopsy. The only exclusionary criterion was the presence of tauopathies other than AD, e.g., argyrophilic grain disease, Niemann Pick disease type C, subacute sclerosing panencephalitis, progressive supranuclear palsy, corticobasal degeneration, or frontotemporal lobar degeneration (Dickson 2009). Demographic and neuropathological staging data for all cases (12 females, 28 males, 41–85 years of age; controls: 6 females, 7 males, 12–77 years of age) are summarized in Table 1.

Tissue Fixation, Embedding, and Sectioning

Brainstems and at least a single hemisphere from all individuals listed in Table 1 were fixed by immersion in a 4%-buffered aqueous solution of formaldehyde for 10–20 days prior to dissection for neuropathological assessment. A set of 2 tissue blocks was excised: The first block was cut at mid-uncal level through medial portions of the temporal lobe and encompassed anterior portions of the hippocampal formation and the parahippocampal gyrus (entorhinal and transentorhinal regions), including the occipitotemporal gyrus and inferior up to and including the superior temporal gyrus. The second block was cut through the occipital lobe perpendicular to the calcarine fissure and included high-order visual association areas (peristriate region), a first order visual association area (parastriate area), and the primary visual field (striate area). The tissue blocks were embedded in polyethylene glycol (PEG 1000, Merck, Carl Roth Ltd, Karlsruhe, Germany) and sectioned on a tetrandler (Jung, Heidelberg, Germany) at 100–300 μm , as previously described (Braak and Braak 1991b; Braak et al. 2006).

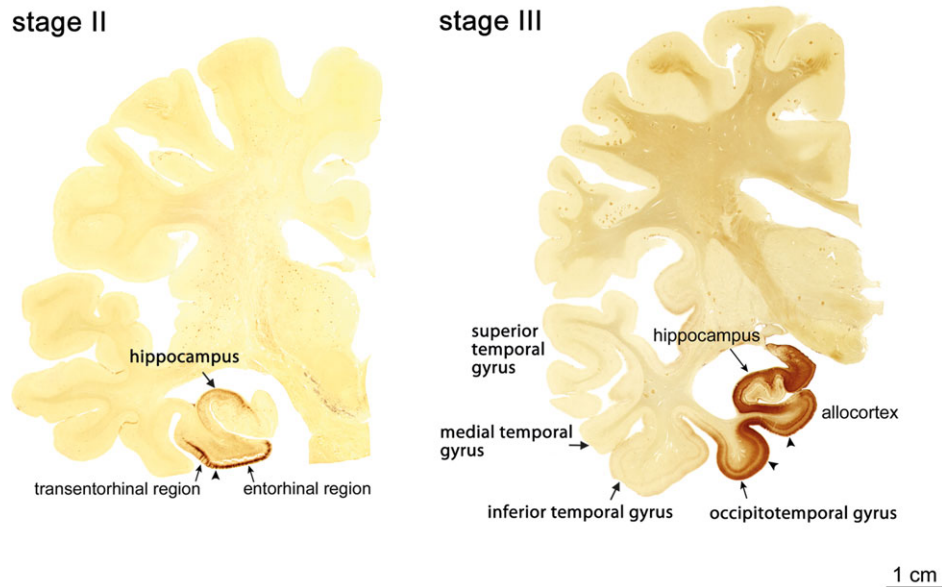


Figure 1. Overview of intraneuronal AT8-immunopositive pathology (NFT stages II and III) in hemisphere sections of 100 μm thickness. The pathology is macroscopically visible in immunostained anteromedial portions of the temporal lobe. Generally, the density of the lesions that are macroscopically visible decreases and tapers off. Here, in a case assigned to NFT stage II (male, 80 years of age), not only the transentorhinal region but also the entorhinal region proper and the hippocampal formation are clearly affected. In a case assigned to NFT stage III (female, 90 years of age), neurofibrillary changes extend beyond the transentorhinal region (arrowheads indicate its borders) into the laterally adjoining neocortex of the occipitotemporal gyrus, whereas the remaining areas of the temporal lobe, particularly the superior temporal gyrus, appear to be intact. However, in the present study, singular isolated large pyramidal cells could be found in these regions. Reproduced with permission from Braak and Del Tredici 2015a. Neuroanatomy and pathology of sporadic Alzheimer's disease. *Adv Anat Embryol Cell Biol* 215:1–162.

Table 1. Demographic and neuropathological data from the cases (N = 40) and controls (N = 13) studied

Case	Age	f/m	NFT	A β	α -syn	1	2	3	4
1	41	f	I	0	0	2	1	1	2
2	50	f	I	0	0	3	1	5	0
3	52	f	I	0	0	3	1	2	1
4	57	m	I	0	0	2	0	0	0
5	57	m	I	0	0	10	4	5	2
6	58	m	I	0	0	1	1	0	0
7	58	m	I	0	0	9	3	11	2
8	62	f	I	1	0	16	2	3	1
9	62	m	I	0	0	6	2	7	2
10	63	f	I	0	0	4	0	0	0
11	65	f	I	0	3	17	7	12	6
12	66	m	I	0	1	1	1	0	0
13	67	m	I	0	0	7	2	9	2
14	68	m	I	0	0	4	4	6	0
15	68	m	I	0	0	1	1	0	0
16	69	m	I	0	0	2	0	2	0
17	69	m	I	0	0	3	1	0	0
18	70	m	I	0	0	2	3	1	1
19	71	m	I	0	0	1	0	0	0
20	71	m	I	0	0	2	1	3	0
21	71	m	I	0	0	3	1	3	0
22	71	m	I	0	0	1	1	2	5
23	76	m	I	0	0	6	1	0	0
24	79	f	I	0	0	1	1	8	0
25	86	m	I	0	0	4	0	0	1
26	61	m	II	0	0	9	3	9	1
27	66	m	II	0	0	7	3	2	1
28	72	m	II	0	0	9	3	7	1
29	73	f	II	0	0	4	1	4	1
30	74	m	II	0	0	6	1	11	1
31	75	m	II	1	5	1	0	4	0
32	75	m	II	1	0	10	4	0	3
33	77	m	II	0	0	7	5	17	4
34	81	m	II	0	0	4	1	1	0
35	72	m	III	0	0	13	1	0	0
36	77	f	III	0	0	1	0	1	0
37	81	f	III	0	0	14	2	4	1
38	85	m	III	1	0	9	2	4	1
39	75	f	IV	2	0	8	3	10	2
40	80	f	IV	1	5	12	8	15	6
Controls									
41	12	m	0	0	0	0	0	0	0
42	16	m	0	0	0	0	0	0	0
43	26	f	0	0	0	0	0	0	0
44	42	m	0	0	0	1	0	0	0
45	49	f	0	0	0	0	0	0	0
46	49	f	0	0	0	0	0	0	0
47	50	f	0	0	0	0	0	0	0
48	60	m	0	0	0	1	0	0	0
49	61	f	0	0	0	0	0	0	0
50	68	m	0	0	0	0	0	0	0
51	69	m	0	0	0	0	0	0	0
52	76	f	0	0	0	0	0	0	0
53	77	m	0	0	0	0	0	0	0

Abbreviations: age—age at death in years; f/m—female/male; NFT—Alzheimer's-related neurofibrillary tangle stages 0–VI (Gallyas silver-iodide staining); A β —Alzheimer's-related amyloid- β deposition phases 0–5 (4G8 immunohistochemistry); α -syn—Parkinson's disease-related neuropathological stages 1–6 (α -synuclein immunohistochemistry). 1–4—4 groups of abnormal AT8-immunopositive inclusions in neocortical layer III and V pyramidal cells (see also Table 2). The number of changed cells in each group is shown in each of the 4 columns.

Staining and Immunocytochemistry

Collections of free-floating sections from all tissue blocks from each case were processed as follows: Following pretreatment with performic acid, pigment-Nissl staining was performed to show the presence and extent of lipofuscin deposits (aldehyde fuchsin) and basophilic material (Darrow red) (Braak and Braak 1991b), silver methods were used to visualize arylphilic neurofibrillary lesions (Gallyas silver-iodide) and A β plaques (Campbell-Switzer) associated with AD (Braak and Braak 1991b; Braak et al. 2006; Hyman et al. 2012).

Immunohistochemistry was performed using the following primary antibodies: (1) the mouse monoclonal antibody PHF-Tau (1:2000; Clone AT8; Pierce Biotechnology, Rockford, IL, USA [Thermo Scientific]) for detection of hyperphosphorylated tau protein in pretangles and in neurofibrillary changes of the Alzheimer type. AT8 recognizes a phosphate-dependent epitope at Serine 202 and Threonine 205 of the tau protein (Goedert et al. 1995). (2) The mouse monoclonal antibody anti-beta-amyloid (1:5000; Clone 4G8; Covance, Dedham, MA, USA) for detection of A β plaque deposition. (3) The mouse monoclonal antibody anti-syn-1 (1:2000; Clone number 42; BD Biosciences, Mountain View, CA, USA) for visualization of Lewy pathology (Braak et al. 2003; Braak and Del Tredici 2009). (4) The rabbit polyclonal antibody that recognizes the N-terminal of the normal nuclear TDP-43 (1:5000; Proteintech, Manchester, UK) for recognition of skein-like cytoplasmic aggregates in amyotrophic lateral sclerosis (Tan et al. 2013). All immunoreactions could be performed on archival tissue stored in formaldehyde (Kaufman et al. 2017).

Tissue sections for immunoreactions were treated for 30 min in a mixture of 10% methanol plus 10% concentrated (30%) H₂O₂ and 80% Tris. Following pretreatment with 100% formic acid for 3 min to facilitate the immunoreactions (anti- β -amyloid), blocking with bovine serum albumin was performed to inhibit endogenous peroxidase and to prevent nonspecific binding. Subsequently, each of the various sets of free-floating sections was incubated for 18 h at 20 °C using the primary antibodies. Subsequent to processing with a corresponding secondary biotinylated antibody (anti-mouse IgG, 1:200; Linaris) for 1.5 h, all immunoreactions were visualized with the avidin-biotin complex (ABC, Vectastain, Vector Laboratories, Burlingame, CA, USA) for 2 h and the chromogen 3,3'-diaminobenzidine tetrahydrochloride (DAB, D5637 Sigma, Taufkirchen, Germany). Omission of the primary antiserum resulted in non-staining. Positive as well as negative control sections were included.

The tissue sections were cleared and mounted in a synthetic resin with a refraction index of 1.58 (Histomount, National Diagnostics, Atlanta, GA, USA). Single sections of both blocks were viewed and neuropathological staging performed with a BX61 microscope (Olympus Optical, Tokyo, Japan). Digital micrographs were taken at different planes using the EFI (extended focal imaging) function as a sharpness projection for stacks of images with the Cell D[®] Imaging Software (Olympus, Münster, Germany). The EFI algorithm extracts the image features with the sharpest contrast from all layers of the stack and merges them into a single image (Supplementary Fig. 1). Pathology was assessed semiquantitatively.

Results

Controls and 40/40 cases showed no intraneuronal somatic TDP-43 aggregates. In contrast to this, 4/40 individuals (#11, 12,

31, 40 in Table 1) displayed Parkinson's disease-associated Lewy neurites and Lewy bodies (Braak et al. 2003; Braak and Del Tredici 2009). In 40/40 individuals and in 2/13 control cases (#44 and 48), AT8-immunopositivity was seen in solitary pyramidal cells of layers III and V in cortical regions distantly located from cortical fields with AT8-immunoreactivity considered to be typical of NFT stages I-IV (Table 1). These abnormal findings either were confined to portions of the involved neuron or filled the entire nerve cell. The AT8-immunoreactivity occurred only in pyramidal neurons, whereas other nerve cell types in their immediate vicinity were intact. The neuropil surrounding the

involved pyramidal cells was devoid of abnormal tau. To facilitate understanding, the AT8-immunoreactive findings can be divided into 4 different groups:

Group 1: To this group belong pyramidal cells, in which only the thickened or swollen distal segments of their basal dendrites and of proximal side branches of the apical dendrite were filled with AT8-immunoreactive abnormal tau (Fig. 2; see also Fig. 5e). These cell processes had a bent appearance (Fig. 2). The skirt-like arrangement of distal segments of the basal dendrites could be followed for some distance, thereby permitting recognition of a central AT8-immunonegative area, around

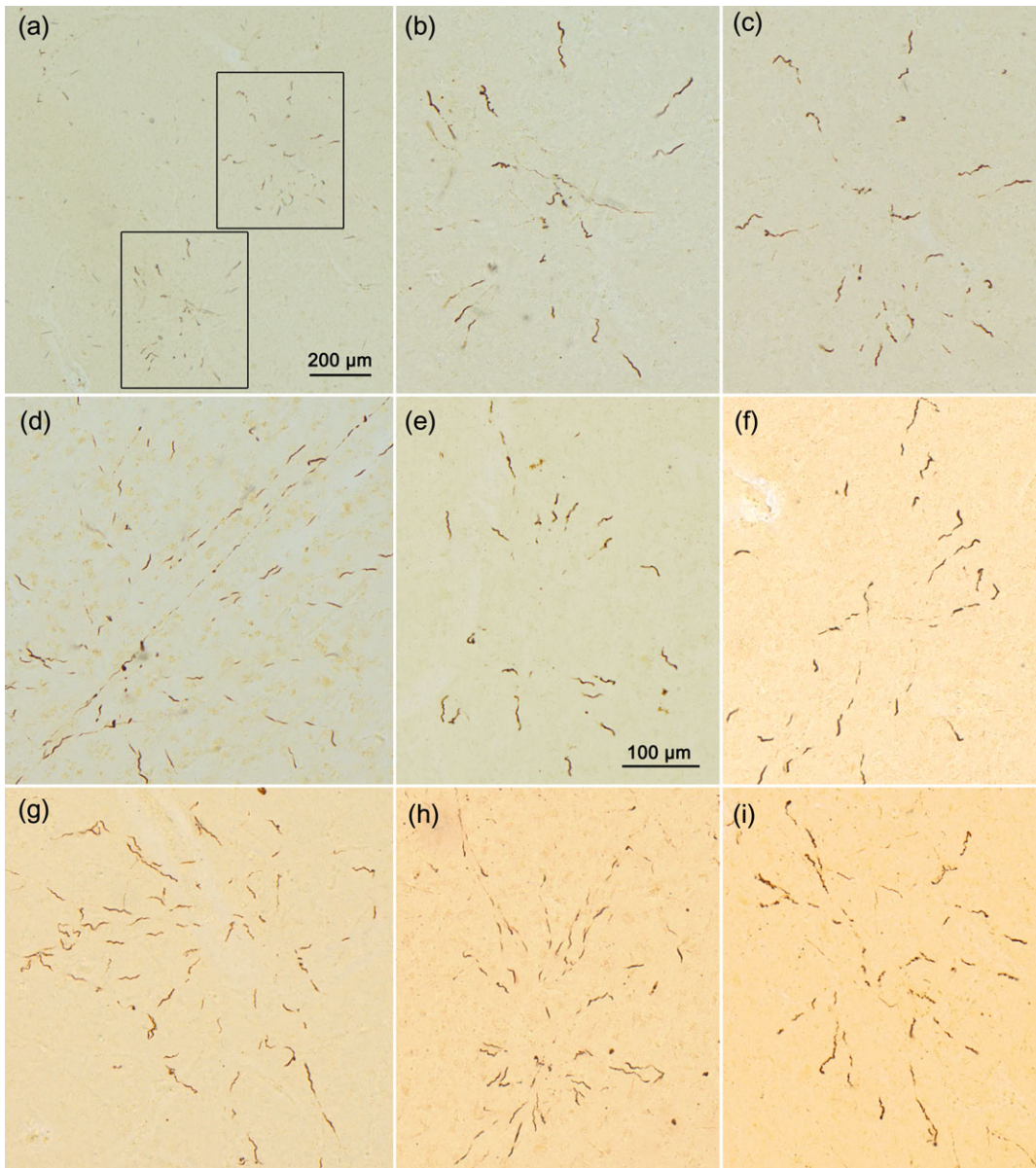


Figure 2. Abnormal tau in distal segments of basal dendrites (Group 1) of isolated pyramidal cells in areas of the neocortex routinely involved only in late NFT stages. (a) Framed areas contain 2 AT8-immunoreactive Group 1 neurons (Case 35, NFT III, superior temporal gyrus, 6 focal planes), which are shown at higher magnification in (b) and (c). The distal dendritic segments appear bent, thickened, and packed with abnormal tau. Notably, the involved distal segments of the basal dendrites form a skirt surrounding a central areal that is immunonegative. Despite the absence of visible physical contacts between the center and the assemblies of immunoreactive dendrites at the perimeter, the impression emerges that they belong to 2 different pyramidal cells in (a), and that they are not bundles of neuronal processes belonging in a random manner to multiple pyramidal cells. (d) The broken diagonal running from the lower left to the upper right of the micrograph (Case 38, NFT III, peristriate region, 8 focal planes) is an AT8-immunoreactive axon that does not belong to the AT8-immunopositive neuron shown. (e) Case 10, NFT I, superior temporal gyrus, 5 focal planes. (f) Case 18, NFT I, superior temporal gyrus, 10 focal planes. (g) Case 11, NFT I, superior temporal gyrus, 10 focal planes. (h) Case 36, NFT III, parastriate region, 10 focal planes. (i) Case 32, NFT II, superior temporal gyrus, 10 focal planes. Scale bar in (e) is also valid for (b-d, f-i). 100- μ m sections.

which the skirt of immunopositive distal dendritic segments was radially oriented (Fig. 2). The AT8-immunopositive dendritic segments appeared to surround an individual (single) pyramidal cell (Fig. 2a) rather than to originate from multiple overlapping pyramidal cells.

Group 2: Other pyramidal cells resembled those in the first group but they also displayed AT8-immunopositive thread-like trailing structures following directly on the thick-caliber distal segments of involved basal dendrites (Fig. 3a–d; see also Fig. 5f). These trailers (or “spokes”) in proximal dendrites had a spatial orientation similar to that of the distal dendritic segments in Group 1 and, again, they surrounded a central area that was immunonegative (Fig. 3a). Alternatively, the central region (or “hub”) was seen to be AT8-immunoreactive but could not be otherwise identified, e.g., as a cell soma (Fig. 3b–d). The calibers of the thread-like trailers in proximal dendrites varied somewhat from cell to cell.

Group 3: To this group belong solitary pyramidal cells that displayed, in addition to the abnormal changes described in

Group 2, the presence of pathological tau in their cell somata and, extending from there, in proximal portions of the apical dendrite (Figs 3e,f, 4a,b; see also Fig. 5g). The apical dendrite was not completely AT8-immunopositive and the tau pathology was not seen to extend into the dendritic terminal tuft (Fig. 4a,b; see also Fig. 5g).

Group 4: The fourth group consists of isolated pyramidal cells whose somata and nearly entire dendritic tree were AT8-immunopositive (Fig. 4c,d). In addition, pathological tau extended into the vertically aligned axon that emanated from the base of the soma (Fig. 4c,d, arrows; see also Fig. 5h). The axon and the axon collaterals filled up with pathological tau in a proximal to distal direction (Fig. 4c, arrows). There were no morphological indications of premature axonal death, nor could abnormalities be detected at the junctures where the axon collaterals began.

Here, 20/40 individuals (#1, 3, 5, 7–9, 11, 13, 18, 22, 26–30, 33, 37–40) displayed all 4 group-related phenomena. By comparison,

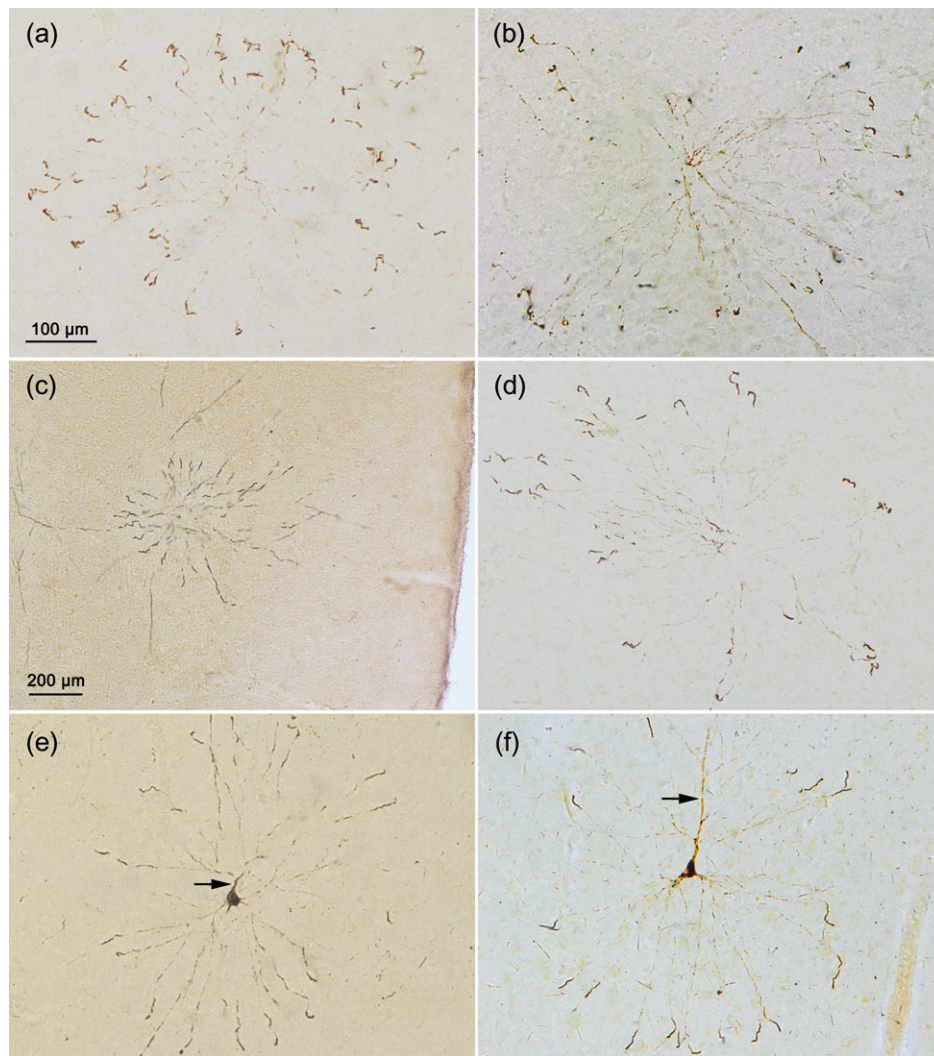


Figure 3. Pathological changes seen in thread-like segments of proximal dendrites (Group 2) as well as in the cell soma and proximal apical dendrite (Group 3) of isolated pyramidal cells in areas of the neocortex routinely involved only in later NFT stages. (a–d). A second group of involved pyramidal neurons resembled those described in Figure 2 but also displayed AT8-immunoreactivity in thread-like segments of proximal dendrites that reach from the thickened distal segments and head towards an AT8-immunonegative center (a) Case 33, NFT II, prefrontal cortex, 9 focal planes; (b) Case 3, NFT I, inferior temporal gyrus, 6 focal planes; (c) Case 5, NFT I, overview of medial temporal gyrus, 9 focal planes; (d) Case 13, NFT I, superior temporal gyrus, 9 focal planes. (e, f) The cell soma and stem of the apical dendrite (arrows) fill up with abnormal tau (Group 3). (e) Case 5, NFT I, superior temporal gyrus, 9 focal planes; (f) Case 27, NFT II, superior temporal gyrus, 9 focal planes. Scale bar in a also applies to (b) and (d–f) 100- μ m sections (b, d, f); 200- μ m sections (a, c, e).

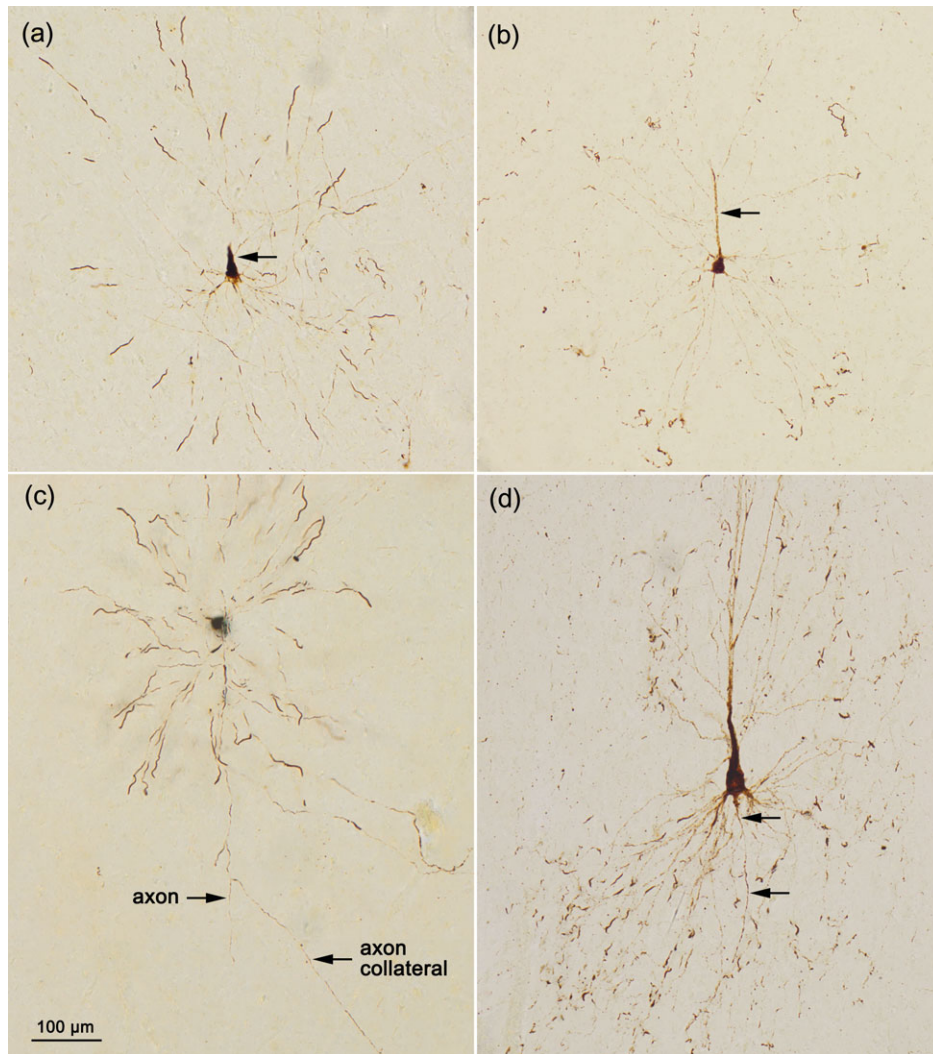


Figure 4. Pathological changes seen in the cell soma and proximal apical dendrite (Group 3) and, additionally, in the axon (Group 4) of isolated pyramidal cells in areas of the neocortex routinely involved only in later NFT stages. (a, b). As in the previous figure (e, f), the cell soma and stem of the apical dendrite (arrows) are filled with abnormal tau (Group 3). Only the axons are AT8-immunonegative. (a) Case 31, NFT II, inferior temporal gyrus, 8 focal planes; (b) Case 27, NFT II, inferior temporal gyrus, 9 focal planes. (c, d) Group 4 pyramidal cells show involvement of nearly their entire dendritic trees and display an AT8-immunopositive axon (arrows at base of the cell soma). No signs of axonal death are detectable. There are no varicosities or visible morphological changes at the junctions of the axon collaterals; (c) Case 33, NFT II, prefrontal cortex, 9 focal planes; (d) Case 16, NFT I, inferior temporal gyrus, 10 focal planes. Scale bar in (c) also applies to (a, b), and (d) 100- μ m sections (a, b, d); 200- μ m section (c).

7/40 (#2, 14, 20, 21, 24, 34, 36) showed the phenomena associated with the first 3 groups, 6/40 persons (#6, 12, 15, 17, 23, 35) showed those associated with the first 2 groups, and 3/40 individuals (#4, 10, 19) displayed only the first group-related phenomena (Table 1, last 4 columns).

We also searched for other abnormal AT8-immunopositive patterns and structures. Thread-like structures that might have been, or belonged to, axons were frequent, but they could not be assigned to a definite pyramidal neuron. Structures that must be mentioned here because of their absence included: (1) thread-like and radially-oriented AT8-immunopositive axons in layers III to V, or AT8-immunopositive axons that ran horizontally through layers I or II; (2) isolated AT8-immunopositive somata and solitary apical dendrites; (3) isolated thread-like AT8-immunoreactive proximal basal dendrites. In addition, we did not see (4) combinations of an AT8-immunopositive axon and an immunopositive soma without an immunoreactive dendritic tree, or (5) a combination of AT8-immunoreactive thread-

like proximal basal dendrites and an immunopositive soma in the absence of immunoreactive distal dendritic segments. Finally, we did not see AT8-immunopositive spiny stellate cells in layer IV of any of the cases studied.

Discussion

In AD, the development of tau pathology is confined to select types of nerve cells of the human brain (Hyman and Gómez-Isla 1994). From its outset, the pathological process consistently involves specific subcortical nuclei and cortical areas and, thereby permitting the distinction of different stages of the intraneuronal lesions (Braak et al. 2006; Duyckaerts et al. 2015; Braak and Del Tredici 2015a, 2015b). From the transentorhinal region (NFT stage I), tau pathology progresses into both the temporal allocortex (i.e., entorhinal region and hippocampal formation, Fig. 1, NFT stage II) and the temporal neocortex (Fig. 1, NFT stage III). This is followed by involvement of

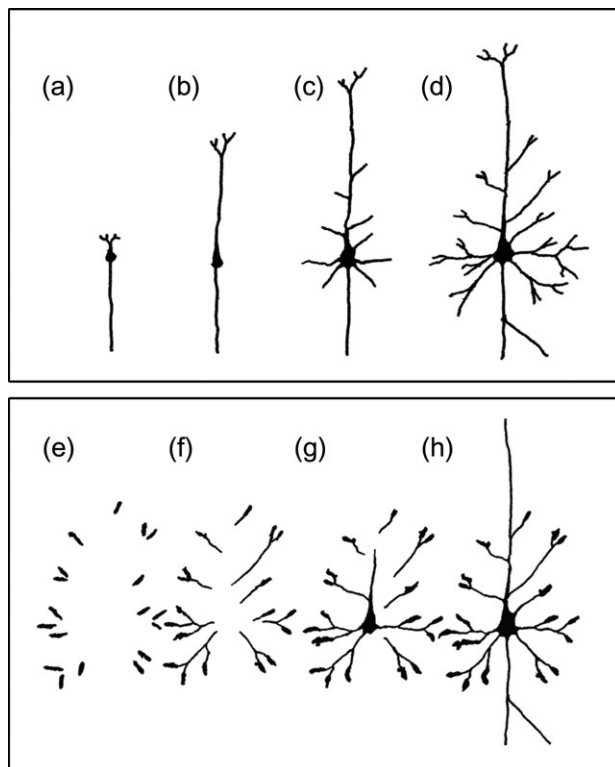


Figure 5. Ontogenetic development of neocortical pyramidal cells (a–d). Generation of the axon (a) is followed by that of a radially-oriented apical dendrite, including its tuft of terminal twigs (b). Next (c), short basal dendrites develop that are complemented by (d) a skirt of later-maturing distal segments of the basal dendrites. Proposed sequential development of AT8 lesions in solitary pyramidal cells located in regions of the neocortex that typically become involved only in later NFT stages (e–h). Distal dendritic segments become filled with AT8-immunoreactive tau aggregates (e). This is followed by the development of immunopositive thread-like structures that emanate from the distal segments into the proximal dendrites leading towards an AT8-immunonegative hub, presumably the cell soma (f). The soma of the pyramidal cell together with proximal portions of the apical dendrite become AT8-immunopositive (g). Finally, the entire pyramidal cell, including its axon, is AT8-immunoreactive (h).

additional regions within the neocortex: parietal and occipital high-order association fields, prefrontal areas (NFT stages IV and V), sensory first order association fields as well as premotor areas (stage V), and, finally, the primary areas (NFT stage VI). The disease-associated symptoms gradually emerge after a protracted preclinical (i.e., clinically silent) phase (Amieva et al. 2008), and it remains unclear why such a slowly, but relentlessly, progressive disease process fails to go into remission (Braak and Del Tredici 2015a).

The uniform topographical or regional distribution pattern of the tau lesions during each NFT stage is in line with the concept put forth by some researchers that spreading of tau pathology within the brain might proceed along axons of involved nerve cells within a given field to hitherto uninvolved nerve cells in other fields (Saper et al. 1987). More recent experiments show that pathogenic forms of tau are capable of seeding and can be transmitted over distances axonally and transsynaptically (Clavaguera et al. 2009; Brundin et al. 2010; Guo and Lee 2011; De Calignon et al. 2012; Liu et al. 2012; Ahmed et al. 2014; Dujardin et al. 2014; Calafate et al. 2015; Lewis and Dickson 2016; Kaufman et al. 2017; Mudher et al. 2017). Applied to the neocortex, this would imply that the

majority of vulnerable pyramidal cells there in AD are not programmed to receive subcortical data or to send it to extracortical regions. Instead, it is more reasonable to surmise that these vulnerable pyramidal cells establish connectivities chiefly between individual neocortical fields (DeFelipe and Farinas 1992; Nieuwenhuys 1994).

Spreading of tau pathology directed by subcortico-cortical pathways is unlikely for 2 reasons: First, during NFT stages I–IV, the only subcortical sources that could possibly transmit seed-containing tau aggregates via axonal transport to neocortical pyramidal cells are the non-thalamic nuclei with diffuse cortical projections (Nieuwenhuys 1996), e.g., the locus coeruleus, upper raphe nuclei, and magnocellular nuclei of the basal forebrain. Ascending and highly ramified projections from these nuclei relay data widely to large fields of the cerebral cortex using chiefly non-junctional varicosities and volume transmission rather than complete (classical) synapses with pre- and postsynaptic densities (Nieuwenhuys 1999, 2000; O'Donnell et al. 2012). Thus, the projections of the subcortical non-thalamic nuclei would not spread the pathology in a selective manner to cortical sites but diffusely to all regions of the cerebral cortex. Such a spreading pattern, however, is inconsistent with the selective regional distribution pattern of abnormal tau during successive NFT stages, where the pathology first involves projection neurons of high-order association fields and prefrontal areas, then those of first order association fields and premotor areas, and only at the very end also those of the primary sensory and motor fields (Fig. 7). Second, the subcortical non-thalamic nuclei are not predominantly supplied with the type of synapse required for transsynaptic seeding-induced transmission or propagation of tau between involved and uninvolved projection neurons, and this may explain why the locus coeruleus, for example, does not display avid tau seeding activity (Kaufman et al. 2018).

Postulate: the 4 Groups of Pathological Changes Correspond to 4 Pathological Sequential Phases

We described above abnormal AT8-immunopositive tau aggregates in solitary pyramidal neurons of layers III and V in the neocortex of individuals with neurofibrillary changes corresponding to NFT stages I–IV. These findings were remarkable in that they usually occur in regions that typically become involved first in later NFT stages. In other words, relative to their NFT stages, the pathologically altered pyramidal cells were far-removed from the affected regions elsewhere that displayed essentially more severe tau pathology. Owing chiefly to their isolated locations, but also because all 4 groups of pathological changes were present in 20/40 individuals and, in an additional 13/40 cases, the abnormalities associated with the first 2 or first 3 groups were seen (Table 1), we postulate that the 4 groups represent 4 phases in a developmental sequence (Table 2, Fig. 5e–h).

Taken together, the 4 proposed phases may represent an initial “reaction” of a previously uninvolved neocortical field to the progressive neuron-to-neuron and transaxonal spread of pathological tau originating from fields with a greater degree of involvement. According to this idea, all newly involved neocortical fields, whether motor or sensory areas, would react similarly to the pathological process regardless of age and gender (Table 1, Figs 2–4). Likewise, the abnormal AT8-immunopositive changes associated with the 4 phases would not be influenced by the presence of the low A β plaque phases or by the absence

Table 2. Four groups of abnormal inclusions in neocortical pyramidal cells of layers III and V as seen in AT8-immunocytochemistry may correspond to 4 sequential phases

Phase	Cellular location of AT8-positive inclusions
1	Distal segments of basal dendrites and side branches of apical dendrites
2	1 + Thread-like structures in proximal dendrites
3	1–2 + Cell soma and proximal segments of apical dendrites
4	1–3 + Axon

The 4 morphological groups of abnormal AT8-positive inclusions in isolated neocortical pyramidal cells of layers III and V may represent 4 sequential phases. All 4 patterns were found in 20/40 cases and could reflect a temporal continuum or trajectory. Notably, when viewed as 4 phases instead of 4 discrete groups, the phases repeat, in reverse order, the phylo- and ontogenetic stages in the development of neocortical pyramidal cells.

of diffuse A β plaques in a given neocortical field (Table 1) (Hyman et al. 2012; Serrano-Pozo et al. 2016).

Bottom-Up Versus Top-down Connectivities in the Neocortex

The various fields of the neocortex evolved phylo- and ontogenetically in an ordered sequence and they also mature in this consecutive order. This phenomenon is traceable in the ontogenetic gradually progressive process of myelination and in the functional maturation of the fields of the neocortex that is linked to myelination (Van der Knaap et al. 1991; Paus et al. 2001; Grydeland et al. 2013) (Figs 6 and 7, blue arrow at far right). The neocortical sensory and motor primary fields were the first to emerge (Fig. 6a) followed by a girdle of adjacent sensory first order association areas and premotor fields (Fig. 6a B). These association areas and premotor fields were supplemented by a profusion of high-order fields (parietal and occipital high-order association areas and prefrontal fields; Fig. 6a C). At the end of this process, the sensory high-order association areas of the basal temporal lobe emerged, which also mature very late (Fig. 6 D), and the last of these is the transitional region between the temporal neo- and allocortex: the transentorhinal cortex (Fig. 6a) (Braak and Del Tredici 2015a, 2015b).

As depicted in Figures 6 and 7, the AD process progresses from D to C, from C to B and, finally, from B to A (Figs 6a–c and 7a–c, red arrow at far left)—in the reverse direction to myelination and to the functional maturation of the cortical fields (retrogenesis) (Braak and Braak 1996; Reisberg et al. 1999, 2002). Among the connections between the various fields of the neocortex are those that establish links from A to B, then B to C and, finally, from C to D (Figs 6 and 7, thin black arrows between boxes indicate bottom-up or so-called “upstream” connectivities that end in layer IV). Others run in the opposite direction: from D to C, from C to B, and from B to A (Figs 6 and 7, thick red arrows between boxes indicate top-down or so-called “downstream” connectivities) (Rockland and Pandya 1979, Barbas and Rempel-Clower 1997; Felleman and van Essen 1991; Pandya 1995; Hochstein and Ahissar 2002). Bottom-up connectivities from A to B mature earlier than the bottom-up connectivities from B to C (or than those from C to D) and before the top-down connectivities from B to A. The top-down connectivities from D to C and from C to B mature only after the connections from C to D attain sufficient maturation.

Bottom-up connectivities terminate preferentially on small projection neurons of the granular layer, namely, the spiny

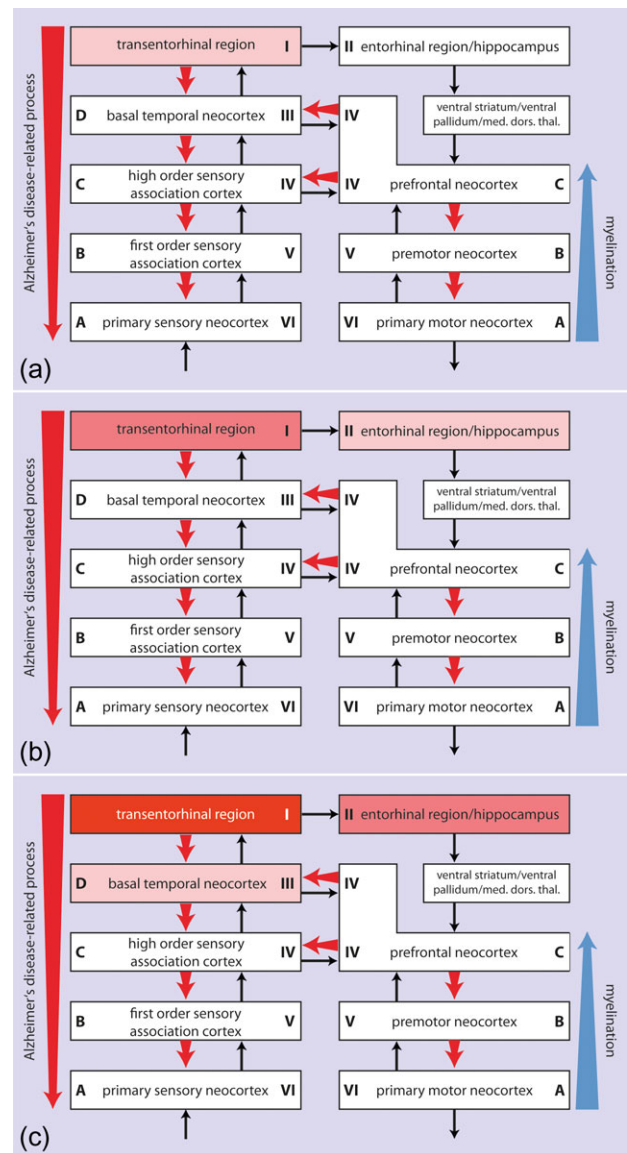


Figure 6. Diagram depicting the possible top-down progression of AD-related tau pathology (NFT stages I–III) along cortico-cortical connections. (a) Cortical tau lesions begin in the transentorhinal region, a transition region between allocortical and neocortical regions of the temporal lobe (NFT stage I). (b) From there, tau pathology progresses into the entorhinal region proper and the hippocampal formation (NFT stage II). (c) The lesions then encroach on the high-order sensory association areas of the basal temporal neocortex (NFT stage III). Notably, whereas top-down projections (thick red arrows) direct the pathological tau process, bottom-up projections (thin black arrows) between involved regions do not develop neurofibrillary pathology in AD. Increasing degrees of shading from light to dark red represent the severity and proposed spread of the lesions.

stellate cells of layer IV. The spiny stellate neurons establish contacts via a short radially-oriented axon to proximal segments of the basal dendrites of pyramidal cells in neocortical layers III and V. In this manner, the spiny stellate cells disseminate the data in an ordered manner to additional projection neurons that belong to a cortical column (Bannister 2005; Barbas 2007).

It is noteworthy that the AD-associated process leaves the spiny stellate cells intact (Braak and Del Tredici 2015a). Moreover, there are no indications that the axonally-interconnected

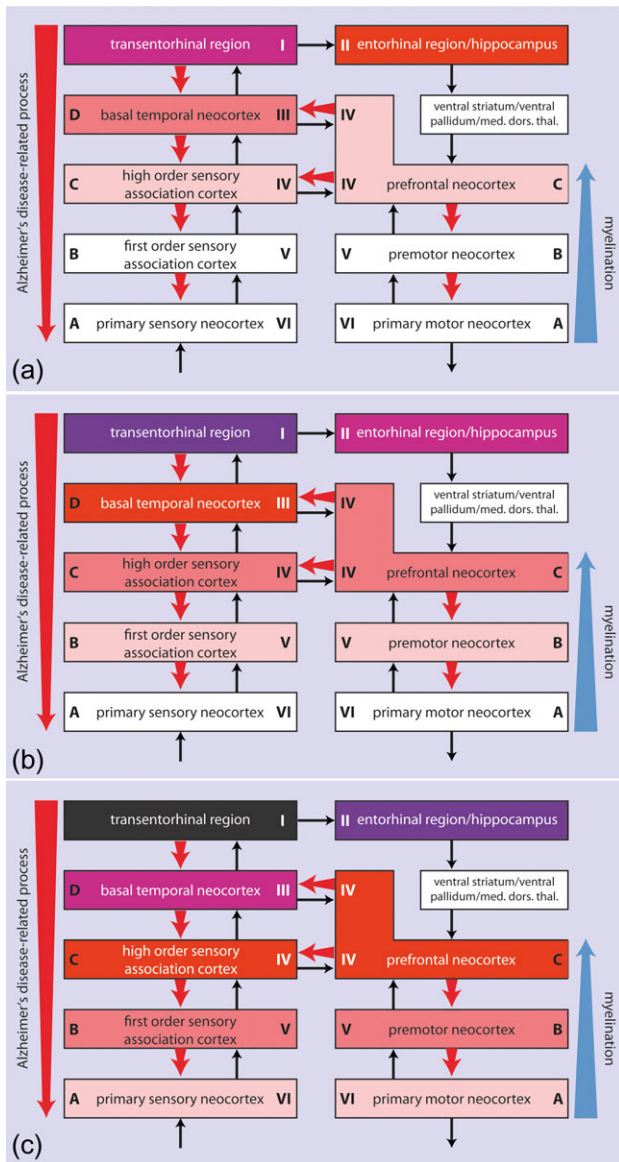


Figure 7. Diagram depicting the possible top-down progression of AD-related tau pathology (NFT stages IV–VI) along cortico-cortical connections. (a) From the high-order sensory association areas of the basal temporal neocortex (NFT stage III), the cortical lesions enter the remaining high-order association fields of the temporal, parietal, and occipital cortices as well as prefrontal areas (NFT stage IV). (b) From there, tau lesions progress into first order sensory association fields and premotor areas (NFT stage V). (c) Finally, tau pathology arrives at the primary fields of the neocortex (NFT stage VI). Once again, top-down projections (thick red arrows) contribute to the spread of the tau pathology, whereas bottom-up projections (thin black arrows) between involved regions do not. Increasing degrees of shading represent the severity and proposed spread of the lesions.

neuronal constituents of a given cortical column become collectively affected. Whether projection neurons with bottom-up connectivities become involved at all during AD is unknown. Cells like the spiny stellate neurons are not among those that are specifically vulnerable and, thus, it is not likely that they could produce tau seeds or axonally transport them. As such, disease progression possibly takes place only by anterograde transport of tau seeds along top-down connectivities (thick red arrows between boxes in Figs 6 and 7). Currently, top-down connectivities

are the focus of ongoing experiments seeking to explain the status of impaired conscious perception during anesthesia (Bullier 2001; Hochstein and Ahissar 2002; Meyer 2011, 2015).

Top-down connections in the neocortex emerged and mature later than the bottom-up connections. Only after B achieves a sufficient degree of maturation and after the connectivities from A to B find their contacts to proximal segments of the basal dendrites of pyramidal cells in neocortical layers III and V, is it possible for connectivities to develop from B to A. However, those in A synapse on pyramidal cells, whose proximal dendrites are already occupied by numerous synapses (*inter alia* belonging to bottom-up projections, or in A thalamo-cortical projections). Nonetheless, during this developmental phase, the dendrites continue sprouting and they produce new distal twigs that in turn provide additional sites for new synapses for the axons that grow into the cortex during this same period.

Tau Seeding in Basal Dendrites and Tau Spreading Along Cortico-cortical Top-Down Connectivities

Here, we shall argue that the proposed phases 1–4 (Fig. 5e–h) repeat, in reverse order, the phylo- and ontogenetic development that takes place in the neocortical pyramidal cells themselves (Marin-Padilla 1992) (Fig. 5a–d). Assuming the hypothesis of a prion-like transsynaptic transmission of abnormal tau is correct, and inasmuch as AT8-immunoreactive tau is confined to distal segments of basal dendrites (phase 1) (Figs 2 and 5e), it follows that abnormal tau could be transmitted only into distal segments of basal dendrites of pyramidal cells located in previously uninvolved neocortical fields. Developmentally, this location makes sense because not only the late-emerging distal dendritic segments of potential recipient pyramidal neurons but also the synapses located on these segments are partially immature (Arendt et al. 1998, 2017; Arendt 2000; Yogeve and Shen 2014). This immaturity could permit the transmission of abnormal proteins.

It has long been thought that the natively soluble and unfolded (“normal”) tau protein is produced in the cell soma and then re-sorted (provided it is fully functional) chiefly into the axonal compartment (von Bergen et al. 2005; Iqbal et al. 2009). There, in mature nerve cells, it helps to stabilize the axonal microtubules (Dotti et al. 1987; Alonso et al. 2008; Zempel et al. 2010). However, the resorting theory is partially inconsistent with our phase 1 findings because it is highly improbable that normal tau can be transferred without a trace and rapidly from the axon of projections neurons into the distant distal dendrites (Thies and Mandelkow 2007; Serrano-Pozo et al. 2011) or that it can be transported rapidly to distal dendrites following renewed tau synthesis in the cell soma (Braak and Del Tredici 2015b). Moreover, none of the nerve cells that become involved during phase 1 display abnormal tau protein in their axons (Figs 2 and 5e). Thus, our findings are in agreement with those of other groups that show “normal” tau is also present in dendrites (Tashiro et al. 1997; Hoover et al. 2010; Ittner et al. 2010; Ittner and Götz 2011; Tai et al. 2012; Merino-Serrais et al. 2013). This implies that, following transsynaptic transmission, it is dendritic tau that would be capable of perpetuating the pathological cascade (Tai et al. 2012; Merino-Serrais et al. 2013).

Ipsilateral top-down projections are said to terminate predominantly in layer I and diffusely in other cortical layers while virtually sparing layer IV (Barbas 2007; Meyer 2015). Our AT8-immunopositive findings in the neocortex are not compatible

with this concept. Notably, abnormal tau does not appear initially either in terminal tufts of apical dendrites (i.e., in layers I or II) or in axons in layers I or II (Fig. 5h). In addition, it appears unlikely that top-down axons from late-maturing neocortical areas would preferentially synapse on the most mature segments of their target cells in subordinate fields.

In phase 2, abnormal tau progresses with thread-like protrusions from AT8-immunoreactive distal segments into the proximal segments headed in the direction of the cell soma (Figs 3a–d and 5f). This finding emphasizes the distinction between distal versus proximal segments of basal dendrites (Häusser and Mel 2003; Gordon et al. 2006; Branco and Häusser 2011; Merino-Serrais et al. 2013). At the same time, it supports the assumption that the synapses located on the proximal segments do not play a role either for abnormal tau propagation or disease progression. As pointed out previously, it is principally the axons arising within the same cortical column (e.g., axons of layer IV spiny stellate cells), which establish the synaptic contacts to the proximal dendrites of the columnar pyramidal cells (Markram 1997; Merino-Serrais et al. 2013). However, the bottom-up connectivities (spiny stellate cells and their axons) remain untouched by the AD process. As such, the abnormal tau changes observed in the thread-like proximal dendrites in phase 2 are not comparable to those seen in the distal dendritic segments of neocortical pyramidal cells (Figs 3a–d and 5f).

The cell soma and the proximal apical dendrite become filled with abnormal tau in phase 3 (Figs 3e,f, 4a,b, and 5g). During the fourth phase, AT8-immunopositive inclusions also develop in the axon (Figs 4c,d and 5h) without light microscopically detectable damage to the axonal cytoskeleton (Fig. 4c,d). These findings are not compatible with the established theory that, following resorting of native tau into the axon, abnormal tau changes begin in the axon. Nor are they compatible with a mechanism of neuron-to-neuron prion-like propagation because the transmission of abnormal tau presupposes the existence of an intact axonal cytoskeleton. We cannot identify the source of abnormal tau in the axon, but it is known that it is initially soluble and uniformly distributed within the axoplasm (Kopelkina et al. 2012). All of this suggests that, even in phase 4, the axon is functional and capable of transporting abnormal (dendritic) tau seeds via intact synapses to interconnected neurons. This situation is superseded by the presence of—apparently less soluble—spindle-like non-argyrophilic tau aggregates in the axon interspersed by AT8-immunonegative axonal segments, and this situation appears to remain stable for a long time because axons containing AT8-immunopositive inclusions are found even in end stage AD cases (Velasco et al. 1998). Thus, the transmission of pathogenic tau seeds may only be possible for a short period, a constraint that could contribute to the interminably protracted disease progression observed in AD. Indeed, most of the neocortical pyramidal cells that develop neurofibrillary lesions survive for many years (Morsch et al. 1999; Braak and Del Tredici 2015a), perhaps because the toxic protein tau (at least in our interpretation) is generated primarily within the *dendritic compartment* and the axonal cytoskeleton is left nearly unimpaired.

It is possible that multiple seed-bearing axons belonging to various previously involved pyramidal neurons all synapse in unison on the ends of all of the basal dendrites of a single intact pyramidal cell in a distant, and heretofore uninvolved, region of the neocortex without synapsing on directly adjacent nerve cells. This scenario, however, appears very improbable in our estimation. Instead, our findings suggest that the terminal axon collaterals of a top-down projection from a single

pyramidal cell synapse on all distal dendritic segments of one and the same target neuron (Figs 2 and 5e). Thus, in our model, spreading of abnormal tau seeds from a seed-bearing axon would occur at multiple synapses located on distal segments of all basal dendrites belonging to a single target neuron (Figs 2 and 5e). Although we cannot explain the mechanisms of this proposed one-to-one selectivity, it could boost the toxic effect of transsynaptically transmitted pathogenic tau, and it could trigger tau seeding in the recipient neuron with a much greater degree of probability than if abnormal tau transmission were to take place across a solitary synaptic contact. Such a mechanism might even be necessary for an effective transmission of abnormal tau and eventually also contribute to the protracted disease course. It might explain as well why the inexorably progressive AD process fails to be subject to spontaneous remission.

Conclusion

This study has several drawbacks: First, it was cross-sectional and not prospective autopsy-controlled (Serrano-Pozo et al. 2011); second, we focused only on the pathology in the large pyramidal cells of layers III and V of the neocortex: These lesions “fit” into what we interpreted as a uniform series of patterns. Nevertheless, it must be pointed out that other types of cortical nerve cells, above all the projection neurons in allocortical regions, display different patterns of AT8-immunopositive lesions (Braak and Del Tredici 2015a) than those presented here.

Not only the new findings in the neocortex but also our interpretation of them here are somewhat unconventional. Nevertheless, from an ontogenetic standpoint, it is conceivable that the late-emerging distal dendritic segments of neocortical pyramidal cells navigate to and establish connections with the axons of late-maturing pyramidal cells in other cortical regions in a highly ordered manner and not randomly (Yogev and Shen 2014). Traditionally, top-down cortico-cortical connections are thought to project in a diffuse manner to numerous and different neuronal constituents in the cortical target areas. However, should our ideas about top-down cortico-cortical pathways prove accurate, then it would be necessary to rethink at least some of the present concepts pertaining not only to the neuropathology of AD but also the structure and function of the human neocortex. In AD, for instance, this means that the contribution of dendritic tau to the pathological process would increase over against that of axonal tau and the microtubule resorting theory. In the human neocortex, this means that not only the bottom-up projections selectively focus their data flow between different neocortical fields (namely, from a given location in the output field to a single column in the target field). The same principle also applies to top-down projections through direct contact by a single axon to only a single projection cell in the target field and to no other projection cell in the target cell's environs.

Supplementary Material

Supplementary material is available at *Cerebral Cortex* online.

Funding

This work was supported by the Hans and Ilse Breuer Foundation (Frankfurt am Main, Germany).

Notes

In commemoration of Korbinian Brodmann (17 November 1868–22 August 1918). We thank the patients and their families who made this study possible, and the Braak Collection (Goethe University Frankfurt am Main), Ms Simone Feldengut (immunoreactions), and Mr David Ewert (University of Ulm) for technical assistance with the graphics. *Conflict of Interest:* None declared.

References

- Ahmed Z, Cooper J, Murray TK, Garn K, McNaughton E, Clark H, Parhizkar S, Ward MA, Cavallini A, Jackson S, et al. 2014. A novel in vivo model of tau propagation with rapid and progressive neurofibrillary tangle pathology: the pattern of spread is determined by connectivity, not proximity. *Acta Neuropathol.* 127:667–683.
- Alafuzoff I, Arzberger T, Al-Sarraj S, Bodi I, Bogdanovic N, Braak H, Bugiani O, Del Tredici K, Ferrer I, Gelpi E, et al. 2008. Staging of neurofibrillary pathology in Alzheimer's disease: a study for the BrainNet Europe Consortium. *Brain Pathol.* 18:484–496.
- Alonso AC, Li B, Grundke-Iqbal I, Iqbal K. 2008. Mechanism of tau-induced neurodegeneration in Alzheimer disease and related tauopathies. *Curr Alzheimer Res.* 5:375–384.
- Amieva H, Le Goff M, Millet X, Orgogozo JM, Pérès K, Barberger-Gateau A, Jacqmin-Gadda H, Dartigues JF. 2008. Prodromal Alzheimer's disease: successive emergence of clinical symptoms. *Ann Neurol.* 64:492–498.
- Amunts K, Zilles K. 2015. Architectonic mapping of the human brain beyond Brodmann. *Neuron.* 88:1086–1107.
- Arendt T. 2000. Alzheimer's disease as a loss of differentiation control in a subset of neurons that retain immature features in the adult brain. *Neurobiol Aging.* 21:783–796.
- Arendt T, Brückner MK, Gertz HJ, Marcova L. 1998. Cortical distribution of neurofibrillary tangles in Alzheimer's disease matches the pattern of neurones that retain their capacity of plastic remodelling in the adult brain. *Neuroscience.* 83:991–1002.
- Arendt T, Stieler J, Ueberham U. 2017. Is sporadic Alzheimer's disease a developmental disorder? *J Neurochem.* 143:396–408.
- Bannister AP. 2005. Inter- and intra-laminar connections of pyramidal cells in the neocortex. *Neurosci Res.* 53:95–103.
- Barbas H. 2007. Specialized elements of orbitofrontal cortex in primates. *Ann NY Acad Sci.* 1121:10–32.
- Barbas H, Rempel-Clower N. 1997. Cortical structure predicts the pattern of corticocortical connections. *Cereb Cortex.* 7:635–646.
- Braak H, Alafuzoff I, Arzberger T, Kretschmar H, Del Tredici K. 2006. Staging of Alzheimer disease-associated neurofibrillary pathology using paraffin sections and immunocytochemistry. *Acta Neuropathol.* 112:389–404.
- Braak H, Braak E. 1991a. Neuropathological staging of Alzheimer-related changes. *Acta Neuropathol.* 82:239–259.
- Braak H, Braak E. 1991b. Demonstration of amyloid deposits and neurofibrillary changes in whole brain sections. *Brain Pathol.* 1:213–216.
- Braak H, Braak E. 1996. Development of Alzheimer-related neurofibrillary changes in the neocortex inversely recapitulates cortical myelogenesis. *Acta Neuropathol.* 92:97–101.
- Braak H, Del Tredici K. 2009. Neuroanatomy and pathology of sporadic Parkinson's disease. *Adv Anat Embryol Cell Biol.* 201:1–119.
- Braak H, Del Tredici K. 2011. Alzheimer's pathogenesis: is there neuron-to-neuron propagation? *Acta Neuropathol.* 121:589–595.
- Braak H, Del Tredici K. 2015a. Neuroanatomy and pathology of sporadic Alzheimer's disease. *Adv Anat Embryol Cell Biol.* 215:1–162.
- Braak H, Del Tredici K. 2015b. The preclinical phase of the pathological process underlying Alzheimer's disease. *Brain.* 138:2814–2833.
- Braak H, Del Tredici K, Rüb U, de Vos RA, Jansen Steur EN, Braak E. 2003. Staging of brain pathology related to sporadic Parkinson's disease. *Neurobiol Aging.* 24:197–210.
- Branco T, Häusser M. 2011. Synaptic integration gradients in single cortical pyramidal cell dendrites. *Neuron.* 69:885–892.
- Brundin P, Melki R, Kopito R. 2010. Prion-like transmission of protein aggregates in neurodegenerative diseases. *Nat Rev Mol Cell Biol.* 11:301–307.
- Bullier J. 2001. Feedback connections and conscious vision. *Trends Cogn Sci.* 5:369–570.
- Calafate S, Buist A, Miskiewicz K, Vijayan V, Daneels G, de Strooper B, de Wit J, Verstreken K, Moechars D. 2015. Synaptic contacts enhance cell-to-cell tau pathology propagation. *Cell Rep.* 11:1–8.
- Clavaguera F, Bolmont T, Crowther RA, Abramowski A, Frank S, Probst A, Fraser G, Stalder AK, Beibel M, Staufenbiel M, et al. 2009. Transmission and spreading of tauopathy in transgenic mouse brain. *Nat Cell Biol.* 11:909–913.
- De Calignon A, Polydoro M, Suárez-Calvet M, William C, Adamowicz DH, Kopeikina KJ, Pitstick R, Sahara N, Ashe KH, Carlson GA, et al. 2012. Propagation of tau pathology in a model of early Alzheimer's disease. *Neuron.* 73:685–697.
- DeFelipe J, Farinas I. 1992. The pyramidal neuron of the cerebral cortex: morphological and chemical characteristics of the synaptic inputs. *Progr Neurobiol.* 39:563–607.
- Dickson DW. 2009. Neuropathology of non-Alzheimer degenerative disorders. *Int J Clin Exp Pathol.* 25:1–23.
- Dotti CG, Banker GA, Binder LI. 1987. The expression and distribution of the microtubule-associated proteins tau and microtubule-associated protein 2 in hippocampal neurons in the rat in situ and in cell culture. *Neuroscience.* 23:121–130.
- Dujardin S, Lécolle K, Caillieuz R, Bégard S, Zommer N, Lachaud C, Carrier S, Dufour N, Aurégan G, Winderickx J, et al. 2014. Neuron-to-neuron wild-type Tau protein transfer through a trans-synaptic mechanism: relevance to sporadic tauopathies. *Acta Neuropathol Commun.* 2:1–14.
- Duyckaerts C, Braak H, Brion J-P, Buée L, Del Tredici K, Goedert M, Halliday G, Neumann M, Spillantini MG, Tolnay M, et al. 2015. PART is part of Alzheimer disease. *Acta Neuropathol.* 129:749–756.
- Felleman DJ, van Essen DC. 1991. Distributed hierarchical processing in the primate cerebral cortex. *Cereb Cortex.* 1:1–47.
- Goedert M, Jakes R, Vanmechelen E. 1995. Monoclonal antibody AT8 recognizes tau protein phosphorylated at serine 202 and threonine 205. *Neurosci Lett.* 189:167–170.
- Gordon U, Polsky A, Schiller J. 2006. Plasticity compartments in basal dendrites of neocortical pyramidal neurons. *J Neurosci.* 26:12717–12726.
- Grydeland H, Walhovd KB, Tamnes CK, Westlye LT, Fjell AM. 2013. Intracortical myelin links with performance variability across the human lifespan: results from T1- and T2-weighter MRI myelin mapping and diffusion tensor imaging. *J Neurosci.* 33:18618–18630.
- Guo JL, Lee VM. 2011. Seeding of normal tau by pathological tau conformers drives pathogenesis of Alzheimer-like tangles. *J Biol Chem.* 286:15317–15331.
- Hochstein S, Ahissar M. 2002. View from the top: Hierarchies and reverse hierarchies in the visual system. *Neuron.* 36:791–804.

- Hoover BR, Reed MN, Su J, Penrod RD, Kotilinek LA, Grant MK, Pitstick R, Carlson GA, Lanier LM, Yuan LL, et al. 2010. Tau mislocalization to dendritic spines mediates synaptic dysfunction independently of neurodegeneration. *Neuron*. 68:1067–1081.
- Hyman BT, Gómez-Isla T. 1994. Alzheimer's disease is a laminar, regional, and neural system specific disease, not a global brain disease. *Neurobiol Aging*. 15:353–354.
- Hyman BT, Phelps CH, Beach TG, Bigio EH, Cairns NJ, Carrillo MC, Dickson DW, Duyckaerts C, Frosch MP, Masliah E, et al. 2012. National Institute on Aging-Alzheimer's Association guidelines for the neuropathologic assessment of Alzheimer's disease. *Alzheimer's Dement*. 8:1–13.
- Häusser M, Mel B. 2003. Dendrites: bug or feature? *Curr Opin Neurobiol*. 13:372–383.
- Iqbal K, Liu F, Gong CX, Alonso C, Grundke-Iqbal I. 2009. Mechanisms of tau-induced neurodegeneration. *Acta Neuropathol*. 118:53–69.
- Ittner LM, Götz J. 2011. Amyloid- β and tau – a toxic pas de deux in Alzheimer's disease. *Nat Rev Neurosci*. 12:65–72.
- Ittner LM, Ke YD, Delerue F, Bi M, Gladbach A, van Eersel J, Wölfing H, Chieng BC, Christie MJ, Napier IA, et al. 2010. Dendritic function of tau mediates amyloid-beta toxicity in Alzheimer's disease mouse models. *Cell*. 142:387–397.
- Kaufman S, Del Tredici K, Thomas TL, Braak H, Diamond MI. 2018. Tau seeding activity begins in the transentorhinal/entorhinal regions and anticipates phospho-tau pathology in Alzheimer's disease and PART. *Acta Neuropathol*. doi:10.1007/s00401-018-1855-6.
- Kaufman S, Thomas TL, Del Tredici K, Braak H, Diamond MI. 2017. Characterization of tau prion seeding activity and strains from formaldehyde-fixed tissue. *Acta Neuropathol Comm*. 5:41.
- Kopelkina KJ, Hyman BT, Spires-Jones TL. 2012. Soluble forms of tau are toxic in Alzheimer's disease. *Transl Neurosci*. 3:223–233.
- Lewis J, Dickson DW. 2016. Propagation of tau pathology: hypotheses, discoveries, and yet unresolved questions from experimental and human brain studies. *Acta Neuropathol*. 131:27–48.
- Liu L, Drouet V, Wu JW, Witter MP, Smith SA, Clelland C, Duff K. 2012. Trans-synaptic spread of tau pathology in vivo. *PLoS One*. 7:e31302.
- Marin-Padilla M. 1992. Ontogenesis of the pyramidal cell of the mammalian neocortex and developmental cytoarchitectonics: a unifying theory. *J Comp Neurol*. 321:223–240.
- Markram H. 1997. A network of tufted layer 5 pyramidal neurons. *Cereb Cortex*. 7:523–533.
- Merino-Serrais P, Benavides-Piccione R, Blazquez-Llorca L, Kastanauskaite A, Rábano A, Avila J, DeFelipe J. 2013. The influence of phospho-tau on dendritic spines of cortical pyramidal neurons in patients with Alzheimer's disease. *Brain*. 136:1913–1928.
- Meyer K. 2011. Primary sensory cortices, top-down projections and conscious experience. *Prog Neurobiol*. 94:408–417.
- Meyer K. 2015. The role of dendritic signaling in the anesthetic suppression of consciousness. *Anesthesiology*. 122:1415–1431.
- Morsch R, Simon W, Coleman PD. 1999. Neurons may live for decades with neurofibrillary tangles. *J Neuropathol Exp Neurol*. 58:188–197.
- Mudher A, Colin M, Dujardin S, Medina M, Dewachter I, Alavi Naini SM, Mandelkow EM, Mandelkow E, Buée L, Goedert M, et al. 2017. What is the evidence that tau pathology spreads through prion-like propagation? *Acta Neuropathol Commun*. 5:99–119.
- Nieuwenhuys R. 1994. The neocortex. An overview of its evolutionary development, structural organization and synaptology. *Anat Embryol (Berl)*. 190:307–337.
- Nieuwenhuys R. 1996. The greater limbic system, the emotional motor system and the brain. *Progr Brain Res*. 107:551–580.
- Nieuwenhuys R. 1999. Structure and organisation of fibre systems. In: Nieuwenhuys R, Ten Donkelaar JH, Nicholson C, editors. *The Central Nervous System of Vertebrates*. Vol 1. Berlin: Springer. p. 113–157.
- Nieuwenhuys R. 2000. Comparative aspects of volume transmission, with sidelight on other forms of intercellular communication. *Prog Brain Res*. 125:49–126.
- O'Donnell J, Zeppenfeld D, McConnell E, Pena S, Nedergaard M. 2012. Norepinephrine: a neuromodulator that boosts the function of multiple cell types to optimize CNS performance. *Neurochem Res*. 37:2496–2512.
- Pandya DN. 1995. Anatomy of the auditory cortex. *Rev Neurol (Paris)*. 151:486–494.
- Paus T, Collins DL, Evans AC, Leonard G, Pike B, Zijdenbos A. 2001. Maturation of white matter in the human brain: a review of magnetic resonance studies. *Brain Res Bull*. 54:255–266.
- Reisberg B, Franssen EH, Hasan SM, Monteiro I, Boksay I, Souren LE, Kenowsky S, Auer SR, Elahi S, Kruger A. 1999. Retrogenesis: clinical, physiologic, and pathologic mechanisms in brain aging, Alzheimer's and other dementing processes. *Eur Arch Psychiatry Clin Neurosci*. 249(Suppl 3):28–36.
- Reisberg B, Franssen EH, Souren LE, Auer SR, Akram I, Kenowsky S. 2002. Evidence and mechanisms of retrogenesis in Alzheimer's and other dementias: management and treatment import. *Am J Alzheimers Dis Other Demen*. 17:2021–2022.
- Rockland KS, Pandya DN. 1979. Laminar origins and terminations of cortical connections of the occipital lobe in the rhesus monkey. *Brain Res*. 179:3–20.
- Saper CB, Wainer BH, German DC. 1987. Axonal and transneuronal transport in the transmission of neurological disease: potential role in system degenerations, including Alzheimer's disease. *Neuroscience*. 23:3893–3898.
- Serrano-Pozo A, Frosch MP, Masliah E, Hyman BT. 2011. Neuropathological alterations in Alzheimer disease. *Cold Spring Harb Perspect Med*. 1:a006189.
- Serrano-Pozo A, Quian J, Muzikansky A, Montine TJ, Frosch MP, Betenksy RA, Hyman BT. 2016. Thal amyloid stages do not significantly impact the correlation between neuropathological change and cognition in the Alzheimer disease continuum. *J Neuropathol Exp Neurol*. 75:516–526.
- Tai HC, Serrano-Pozo A, Hashimoto T, Frosch MP, Spires-Jones TL, Hyman BT. 2012. The synaptic accumulation of hyperphosphorylated tau oligomers in Alzheimer disease is associated with dysfunction of the ubiquitin-proteasome system. *Am J Pathol*. 181:14263–14265.
- Tan RH, Shepherd CE, Kril JJ, McCann H, McGeachie A, McGinley C, Affleck A, Halliday GM. 2013. Classification of FTLD-TDP cases into pathological subtypes using antibodies against phosphorylated and non-phosphorylated TDP43. *Acta Neuropathol Comm*. 1:33.
- Tashiro K, Hasegawa M, Ihara Y, Iwatsubo T. 1997. Somatodendritic localization of phosphorylated tau in neonatal and adult rat cerebral cortex. *Neuroreport*. 8:2797–2801.

- Thies E, Mandelkow EM. 2007. Missorting of tau in neurons causes degeneration of synapses that can be rescued by kinase MARK2/Par-1. *J Neurosci.* 27:2896–2907.
- van der Knaap MS, Valk J, Bakker CJ, Schooneveld M, Faber JA, Willemsse J, Gooskens RH. 1991. Myelination as an expression of the functional maturity of the brain. *Dev Med Child Neurol.* 33:849–857.
- Velasco ME, Smith MA, Siedlak SI, Nunomura A, Perry G. 1998. Striation is the characteristic neuritic abnormality in Alzheimer disease. *Brain Res.* 813:329–333.
- von Bergen M, Barghorn S, Biernat J, Mandelkow EM, Mandelkow E. 2005. Tau aggregation is driven by a transition from random coil to beta sheet structure. *Biochim Biophys Acta.* 1739:158–166.
- Yogev S, Shen K. 2014. Cellular and molecular mechanisms of synaptic specificity. *Annu Rev Cell Dev Biol.* 30:417–437.
- Zempel H, Thies E, Mandelkow E, Mandelkow EM. 2010. A β oligomers cause localized Ca²⁺ elevation, missorting of endogenous tau into dendrites, tau phosphorylation, and destruction of microtubules and spines. *J Neurosci.* 30:11938–11950.
- Zilles K, Amunts K. 2012. Architecture of the cerebral cortex. In: Mai JK, Paxinos G, editors. *The Human Nervous System*. 3rd ed. Amsterdam: Elsevier. p. 836–895.